Electronic Supplementary Information for

A supramolecular cascade assembly with a two-step sequential energy transfer process for enhanced photocatalytic performance

Guang-Lu Li, Kai-Kai Niu, Xuan-Zong Yang, Hui Liu, Shengsheng Yu* and Ling-Bao Xing*

School of Chemistry and Chemical Engineering, Shandong University of Technology, Zibo 255000, Shandong Province, P. R. China

*Corresponding author: Tel./fax: +86 533 2781664. E-mail: ssyu@sdut.edu.cn; lbxing@sdut.edu.cn.

Experimental

Materials: Unless specifically mentioned, all chemicals are commercially available and were used as received.

Characterizations

^{1}H NMR and ^{13}C NMR spectra were recorded on a Bruker Avance 400 spectrometer (400 MHz) at 298 K, and the chemical shifts (δ) were expressed in ppm, and *J* values were given in Hz. UV-vis spectra were obtained on a Shimadzu UV-1601PC spectrophotometer in a quartz cell (light path 10 mm) at 298 K. Steady-state fluorescence measurements were carried out using the FLS5 Steady-State/Transient Fluorescence Spectrometer. Dynamic light scattering (DLS) and zeta potential are measured on Malvern Zetasizer Nano ZS90. Transmission electron microscopy (TEM) images were obtained on a JEM 2100 operating at 120 kV. Samples for TEM measurement was prepared by dropping the mixed aqueous solution on a carbon-coated copper grid (300 mesh) and drying by slow evaporation. Hamamatsu absolute quantum yield measuring instrument Quantaurus-QY was used to obtain fluorescence quantum yields. The time-resolved fluorescence decay curve was obtained by the FLS5 Steady-State/Transient Fluorescence Spectrometer. Photoluminescence spectra was recorded by FLS5 equipped.

Energy-transfer efficiency calculation

The energy-transfer efficiency (Φ_{ET}) was calculated from excitation fluorescence spectra through the equation S1:

$$\Phi_{ET} = 1\text{-}I_{DA}/I_{D} \quad (S1)$$

Where I_{DA} and I_{D} are the fluorescence intensities of the emission of PATT-CB[7]-SBE-β-CD+EY or PATT-CB[7]-SBE-β-CD+EY+SR101 (acceptor), and PATT-CB[7]-SBE-β-CD or PATT-CB[7]-SBE-β-CD+EY (donor) respectively, when excited at 313 nm. The energy-transfer efficiency (Φ_{ET}) was calculated as 14% and 20% in an aqueous environment, measured under the condition of [PATT] = 1.0×10^{-5} mol/L, CB[7] = 4.0×10^{-5} mol/L, [SBE-β-CD] = 1.6×10^{-5} mol/L, EY= 7.5×10^{-7} mol/L, SR101= 1.1×10^{-6} mol/L.

Antenna effect calculation

The Antenna effect was calculated based on the excitation spectra using equation S2:

$$\text{Antenna effect} = (I_{DA,313}\text{-}I_{D,313}) / I_{DA,516/580} \quad (S2)$$

Where I_{DA} and I_{D} are the fluorescence intensities of the emission of PATT-CB[7]-SBE-β-CD+EY,

or PATT-CB[7]-SBE-β-CD+EY+SR101 (acceptor) and PATT-CB[7]-SBE-β-CD or PATT-CB[7]-SBE-β-CD+EY (donor) respectively, when excited at 313 nm. The antenna effect value was calculated as 10.3 and 11.4 in water, measured under the condition of [PATT] = 1.0×10^{-5} mol/L, CB[7] = 4.0×10^{-5} mol/L, [SBE-β-CD] = 1.6×10^{-5} mol/L, EY= 7.5×10^{-7} mol/L, SR101= 1.1×10^{-6} mol/L.

General procedure for the aerobic oxidation reaction of *N*-phenyltetrahydroisoquinoline:

The *N*-phenyltetrahydroisoquinoline or its derivatives (0.20 mmol) was added in the newly produced solution of PATT-CB[7]-SBE-β-CD+EY+SR101 (0.6 mol%). The mixture was irradiated with 360-365 nm LED (10 W) at room temperature for 36 h. Then, the mixture was extracted with dichloromethane and dried with anhydrous Na_2SO_4. The organic solution was concentrated in a vacuum and purified by rapid column chromatography to obtain the corresponding products.

General procedure for photooxidation reactions of benzylamine:

The benzylamine (0.20 mmol) was added in the newly produced solution of PATT-CB[7]-SBE-β-CD+EY+SR101 (1 mol%). The mixture was irradiated with 360-365 nm LED (10 W) at room temperature for 24 h. Then, the mixture was extracted with ethyl acetate and dried with anhydrous Na_2SO_4. The organic solution was concentrated in a vacuum and purified by rapid column chromatography to obtain the corresponding products.

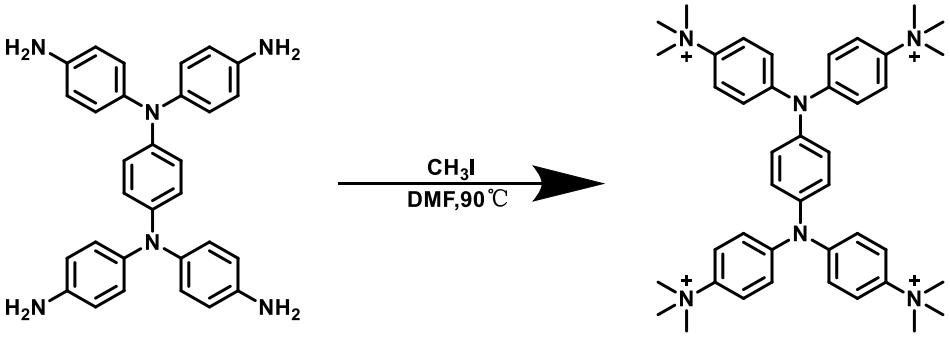

Scheme S1 Synthetic route of PATT.

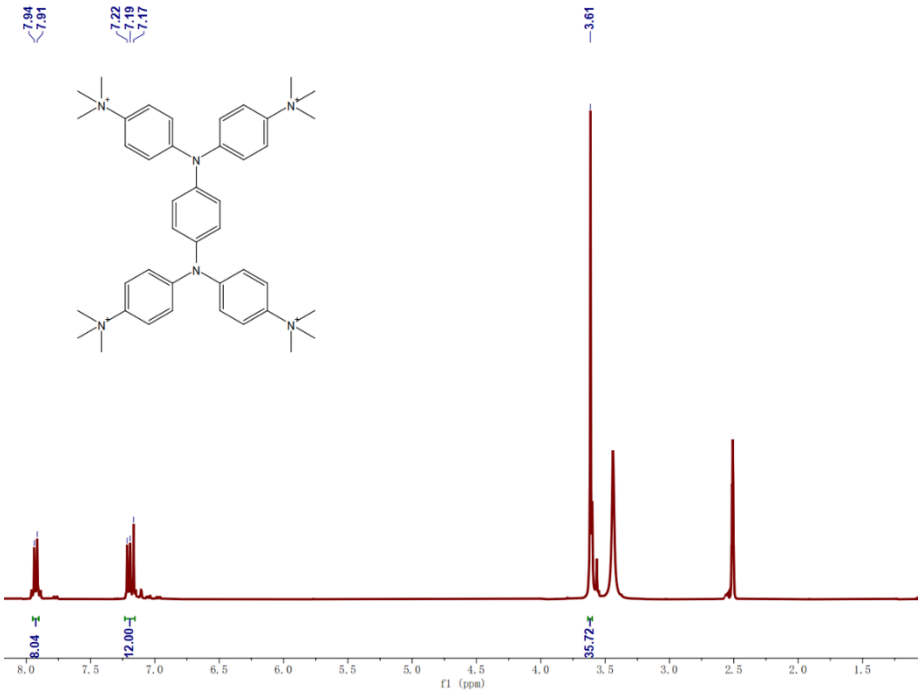

Fig. S1 ^{1}H NMR spectra of PATT in DMSO-d_6.

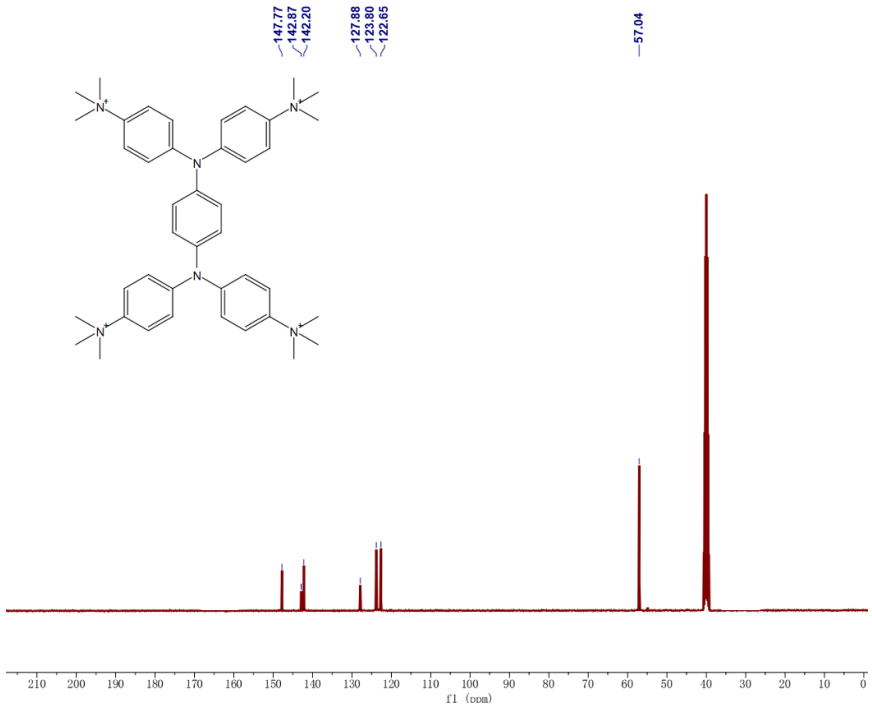

Fig. S2 ^{13}C NMR spectra of PATT in DMSO-d_6.

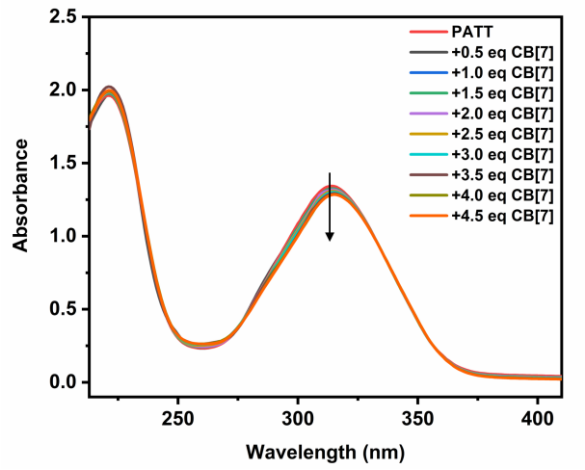

Fig. S3 UV-vis absorption spectra of PATT with the addition of CB[7] ([PATT] = 1.0×10^{-5} mol/L, CB[7] = 4.0×10^{-5} mol/L).

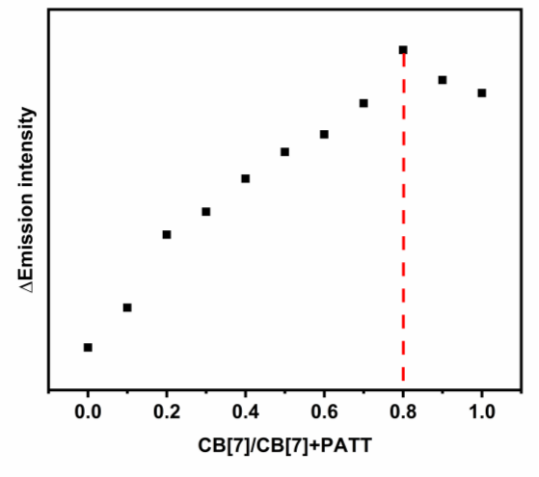

Fig. S4 The Job's plot of PATT and CB[7] system in the aqueous solution.

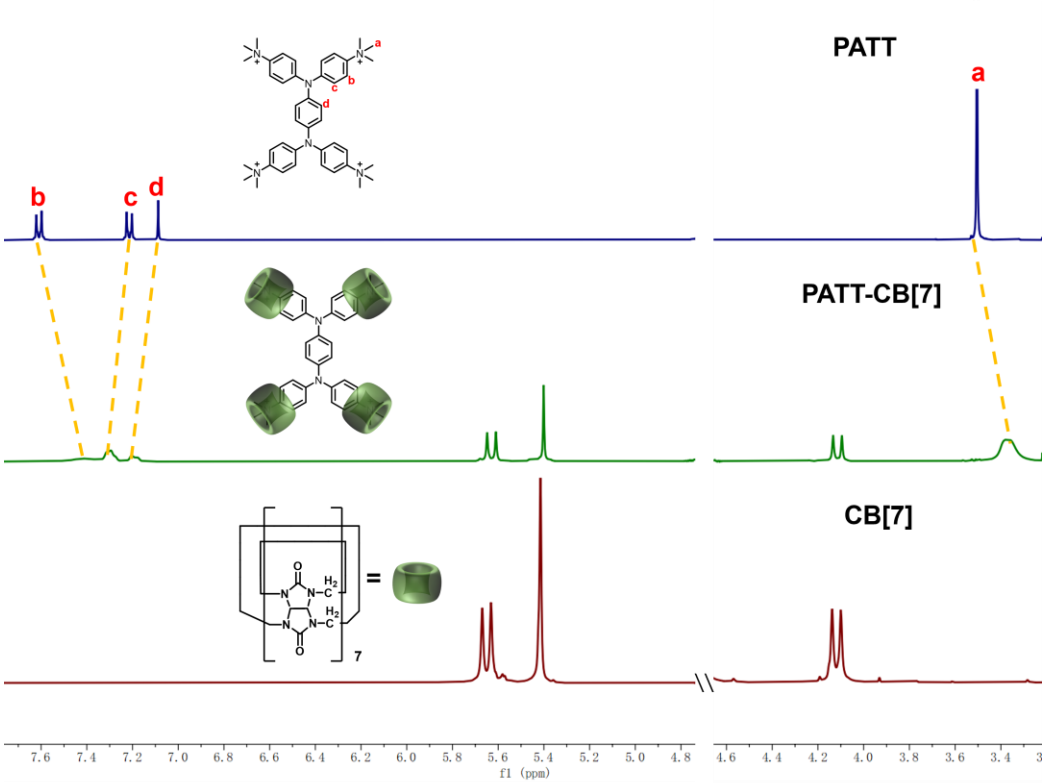

Fig. S5 ^{1}H NMR spectra of PATT in the presence of 4.0 equiv. CB[7] in D_2O ([PATT] = 1.0×10^{-5} mol/L, CB[7] = 4.0×10^{-5} mol/L, [PATT]+[CB[7]] = 1.0×10^{-5} M).

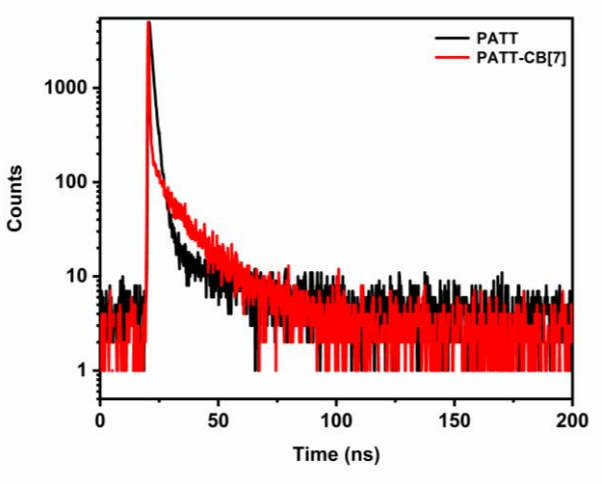

Fig. S6 Time-resolved fluorescence decay curves of PATT and PATT-CB[7] ([PATT] = 1.0×10^{-5} mol/L, CB[7] = 4.0×10^{-5} mol/L).

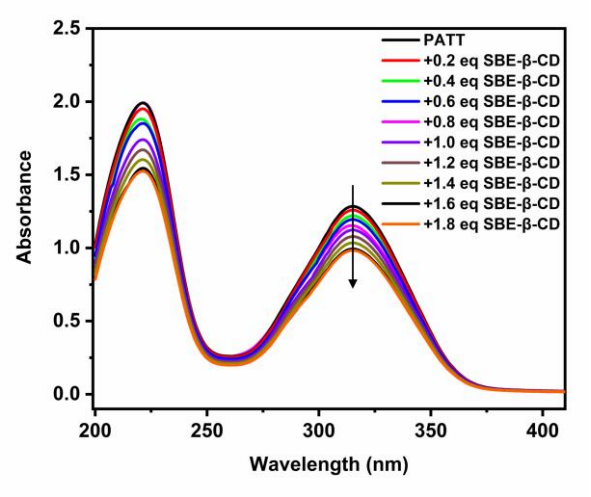

Fig. S7 UV-vis absorption spectra of PATT-CB[7]with the addition of SBE-β-CD ([PATT] = 1.0 × 10^{-5} mol/L, CB[7] = 4.0 × 10^{-5} mol/L, [SBE-β-CD] = 1.6 × 10^{-5} mol/L).

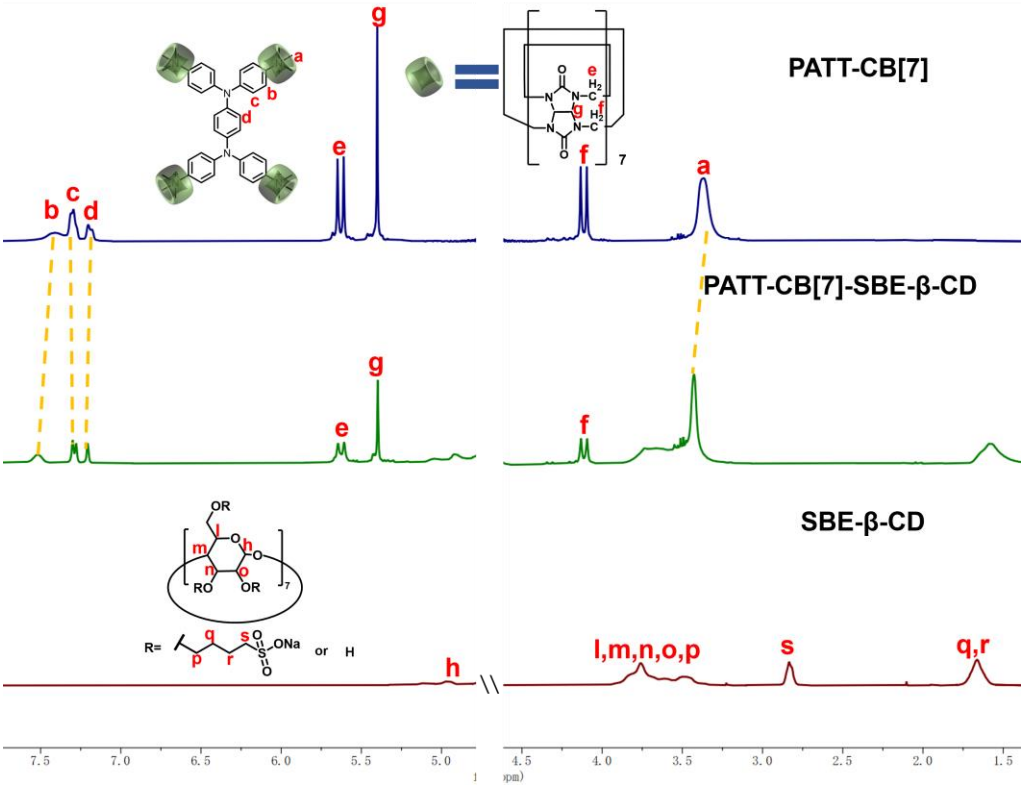

Fig. S8 ^{1}H NMR spectra of PATT-CB[7] in the presence of 1.6 equiv. SBE-β-CD in D_2O ([PATT] = 1.0×10^{-5} mol/L, CB[7] = 4.0×10^{-5} mol/L, [SBE-β-CD] = 1.6×10^{-5} mol/L).

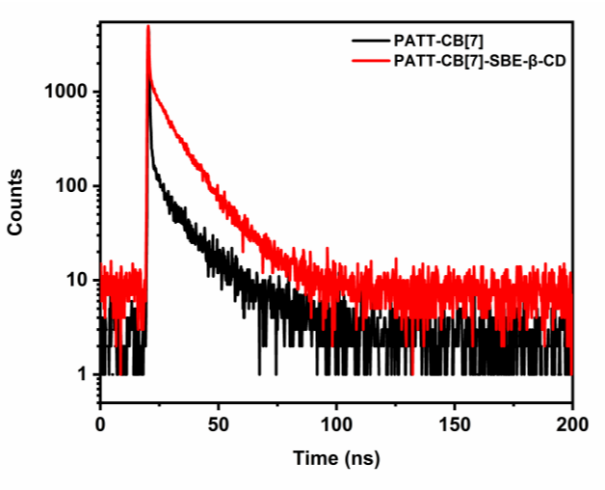

Fig. S9 Time-resolved fluorescence decay curves of PATT-CB[7] and PATT-CB[7]-SBE-β-CD ([PATT] = 1.0×10^{-5} mol/L, CB[7] = 4.0×10^{-5} mol/L, [SBE-β-CD] = 1.6×10^{-5} mol/L).

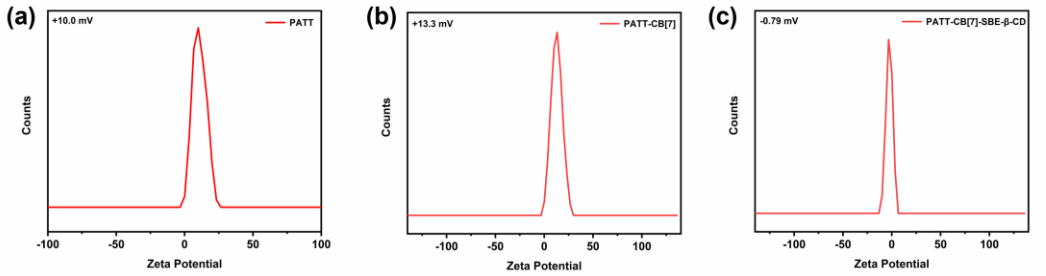

Fig. S10 Zeta potential of (a) PATT, (b) PATT-CB[7], and (c) PATT-CB[7]-SBE-β-CD ([PATT] = 1.0×10^{-5} mol/L, CB[7] = 4.0×10^{-5} mol/L, [SBE-β-CD] = 1.6×10^{-5} mol/L).

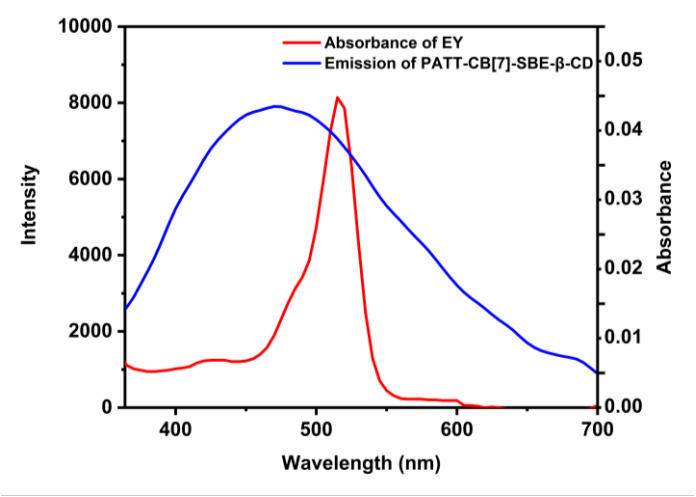

Fig. S11 Fluorescence emission spectra of PATT-CB[7]-SBE-β-CD and UV-vis absorption spectra of EY.

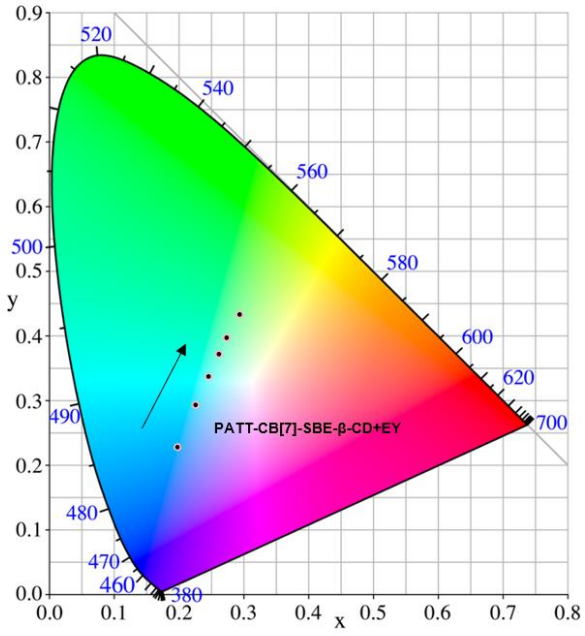

Fig. S12 CIE chromaticity coordinates of PATT-CB[7]-SBE-β-CD at different concentrations of EY (from 0 to 0.05 equiv.) ([PATT] = 1.0×10^{-5} mol/L, CB[7] = 4.0×10^{-5} mol/L, [SBE-β-CD] = 1.6×10^{-5} mol/L).

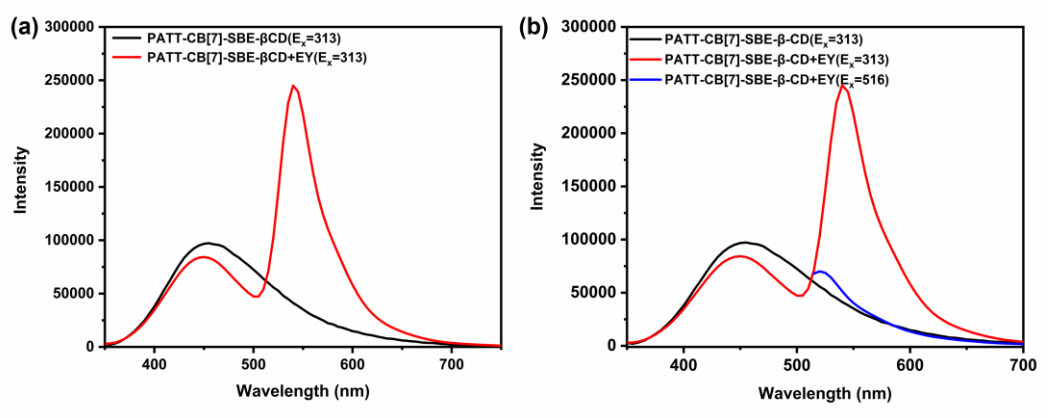

Fig. S13 (a) Fluorescence emission spectra of PATT-CB[7]-SBE-β-CD and PATT-CB[7]-SBE-β-CD+EY; (b) Fluorescence emission spectra of PATT-CB[7]-SBE-β-CD +EY (the red line), PATT-CB[7]-SBE-β-CD+EY (the blue line), PATT-CB[7]-SBE-β-CD (the black line) ([PATT] = 1.0×10^{-5} mol/L, CB[7] = 4.0×10^{-5} mol/L, [SBE-β-CD] = 1.6×10^{-5} mol/L, EY= 5.0×10^{-7} mol/L).

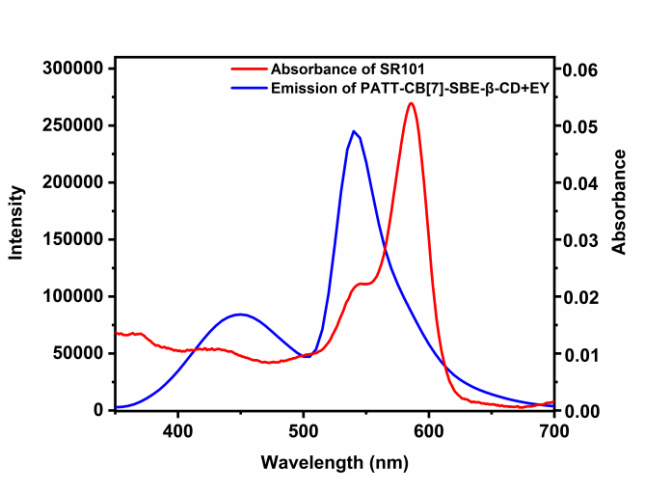

Fig. S14 Fluorescence emission spectra of PATT-CB[7]-SBE-β-CD+EY and UV-vis absorption spectra of SR101.

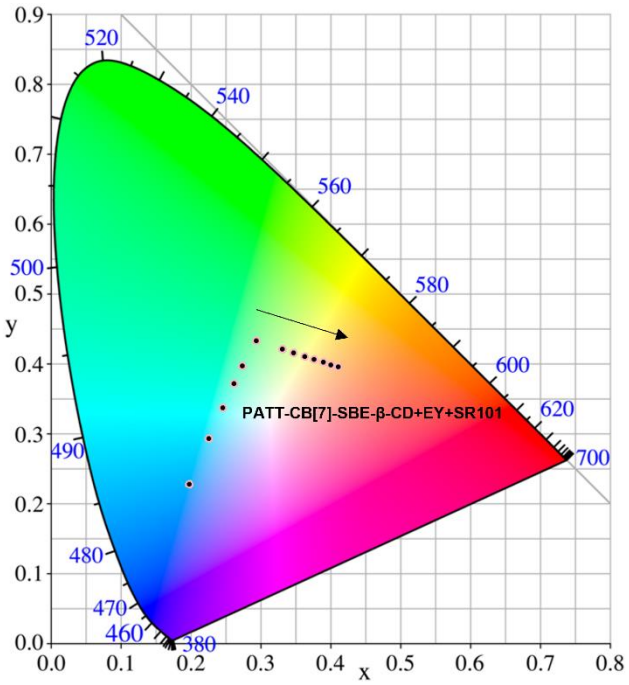

Fig. S15 CIE chromaticity coordinates of PATT-CB[7]-SBE-β-CD+EY at different concentrations of SR101 (from 0 to 0.07 equiv.) ([PATT] = 1.0×10^{-5} mol/L, CB[7] = 4.0×10^{-5} mol/L, [SBE-β-CD] = 1.6×10^{-5} mol/L, EY= 5.0×10^{-7} mol/L).

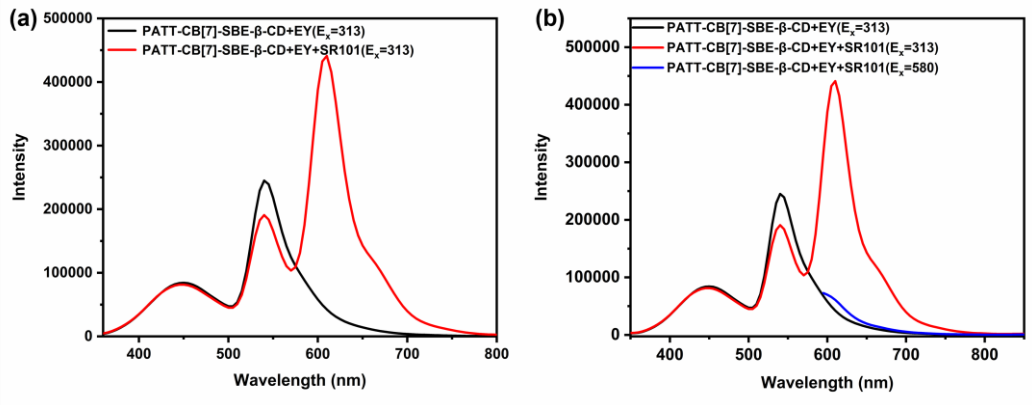

Fig. S16 (a) Fluorescence emission spectra of PATT-CB[7]-SBE-β-CD+EY and D PATT-CB[7]-SBE-β-CD+EY+SR101; (b) Fluorescence emission spectra of PATT-CB[7]-SBE-β-CD +EY+SR101 (the red line), PATT-CB[7]-SBE-β-CD+EY+SR101 (the blue line), PATT-CB[7]-SBE-β-CD+EY (the black line) ([PATT] = 1.0×10^{-5} mol/L, CB[7] = 4.0×10^{-5} mol/L, [SBE-β-CD] = 1.6×10^{-5} mol/L, EY= 5.0×10^{-7} mol/L, SR101= 7.0×10^{-7} mol/L).

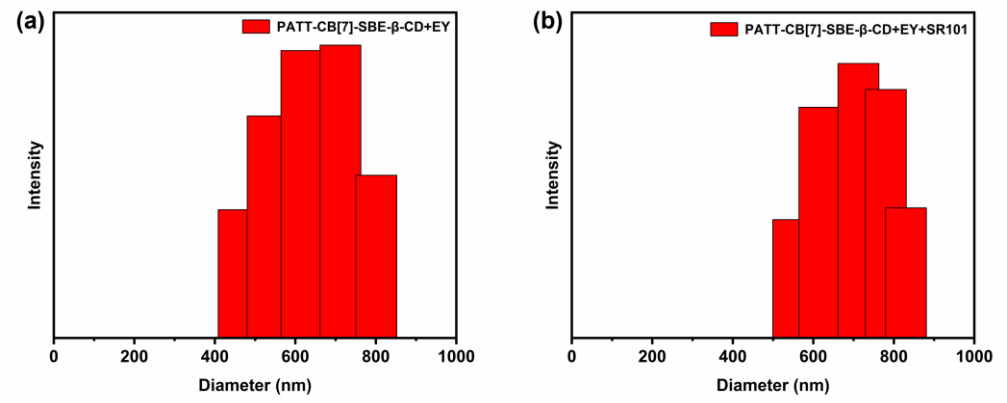

Fig. S17 DLS of (a) PATT-CB[7]-SBE-β-CD+EY and (b) PATT-CB[7]-SBE-β-CD+EY+SR101 ([PATT] = 1.0×10^{-5} mol/L, CB[7] = 4.0×10^{-5} mol/L, [SBE-β-CD] = 1.6×10^{-5} mol/L, EY= 5.0×10^{-7} mol/L, SR101= 7.0×10^{-7} mol/L).

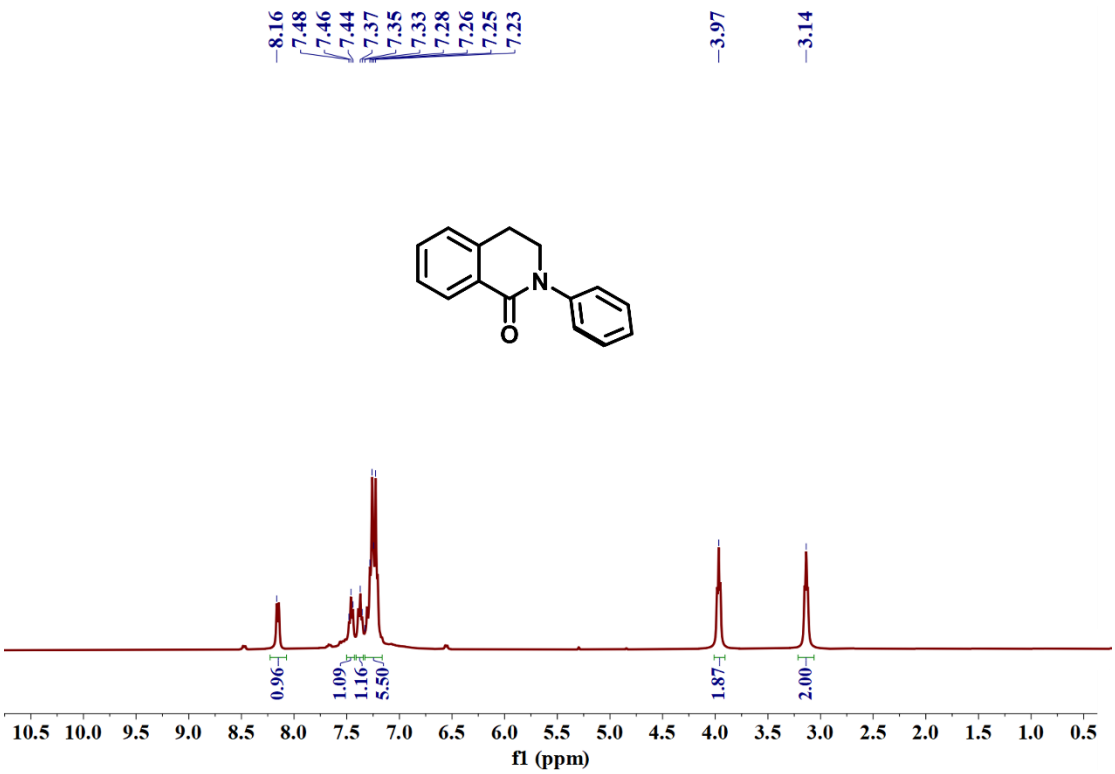

Fig. S18 ^{1}H NMR spectra of **2a** in $CDCl_3$.

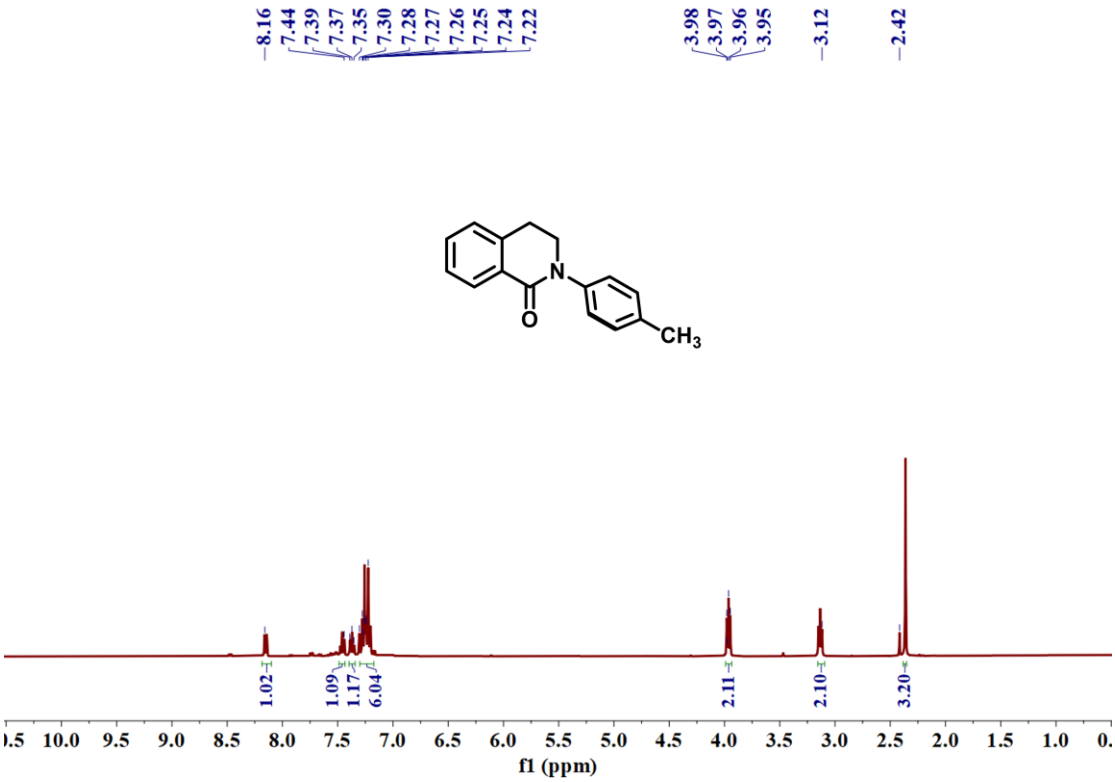

Fig. S19 ^{1}H NMR spectra of **2b** in $CDCl_3$.

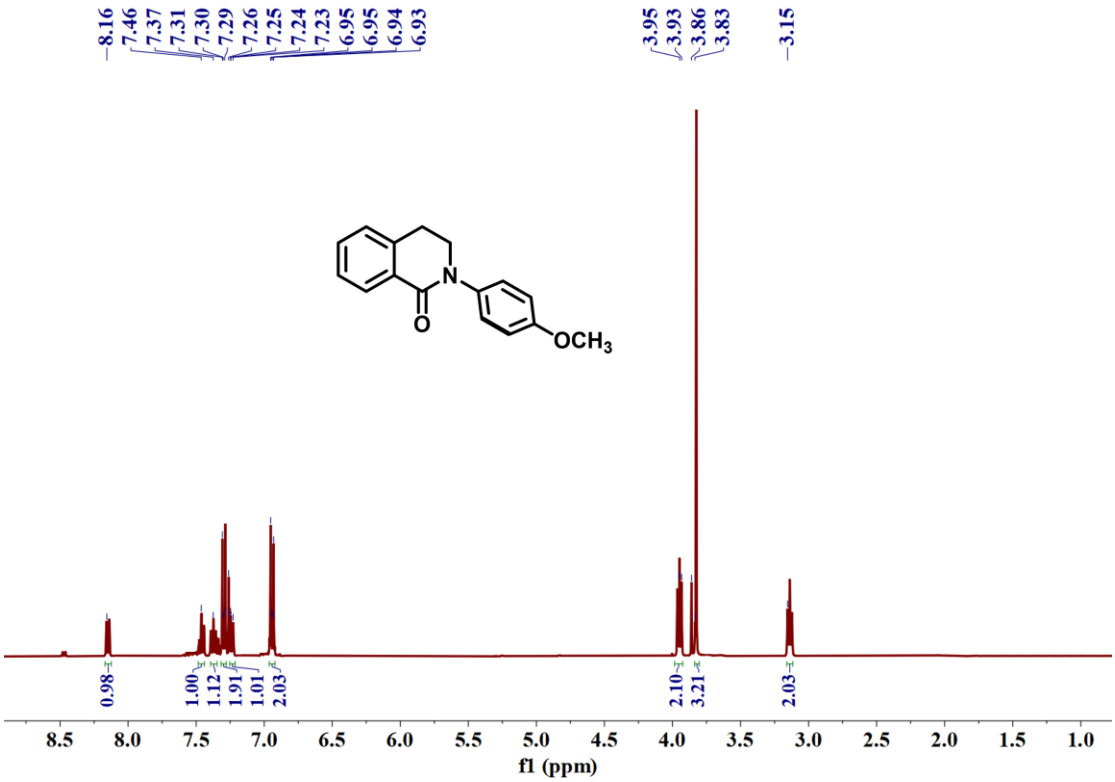

Fig. S20 ^{1}H NMR spectra of **2c** in $CDCl_3$.

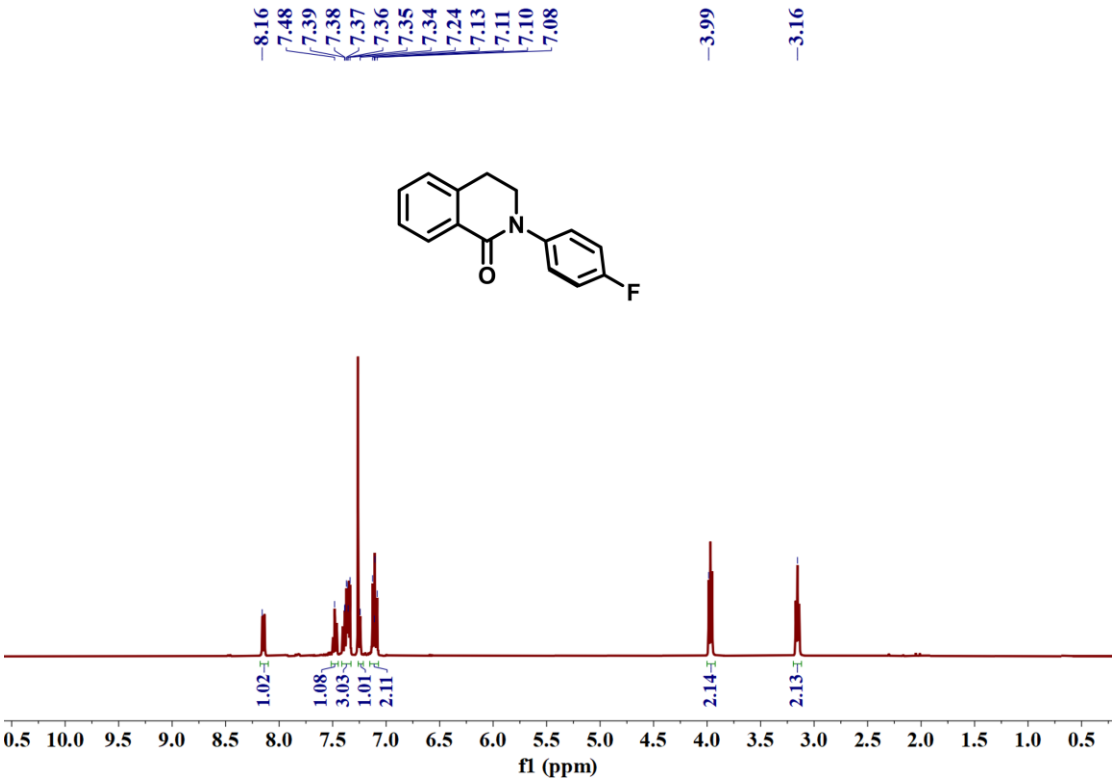

Fig. S21 ^{1}H NMR spectra of **2d** in $CDCl_3$.

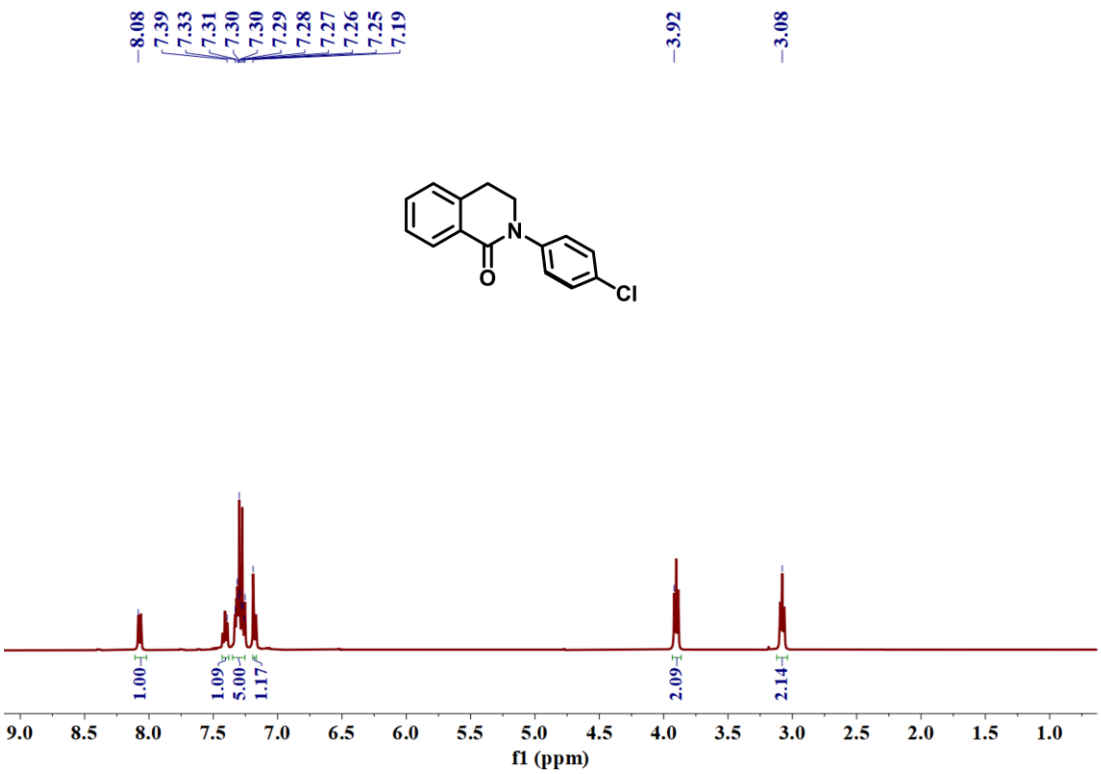

Fig. S22 ^{1}H NMR spectra of **2e** in $CDCl_3$.

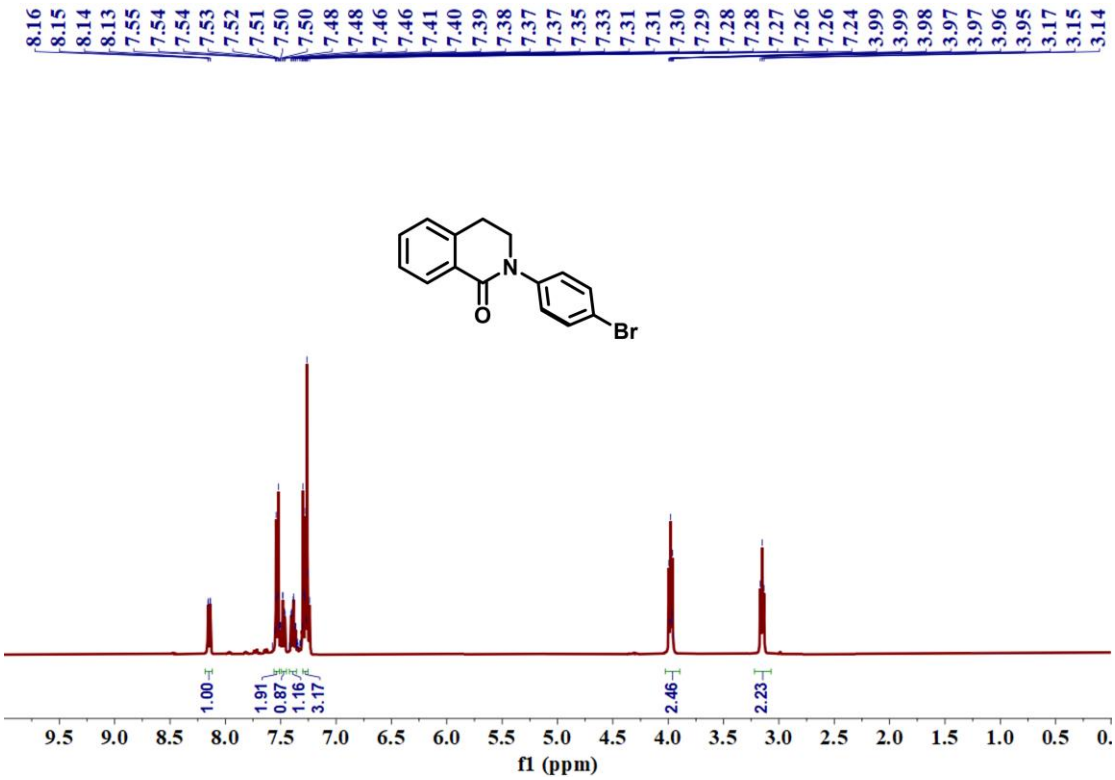

Fig. S23 ^{1}H NMR spectra of **2f** in $CDCl_3$.

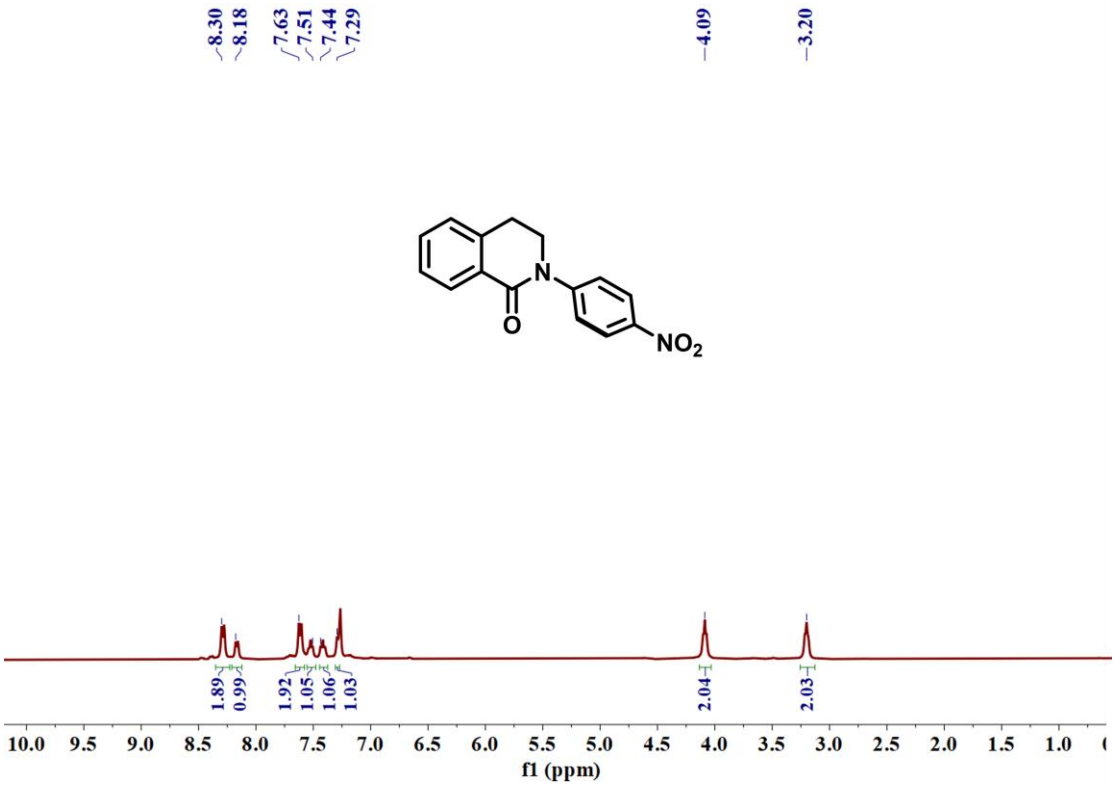

Fig. S24 ^{1}H NMR spectra of **2g** in $CDCl_3$.

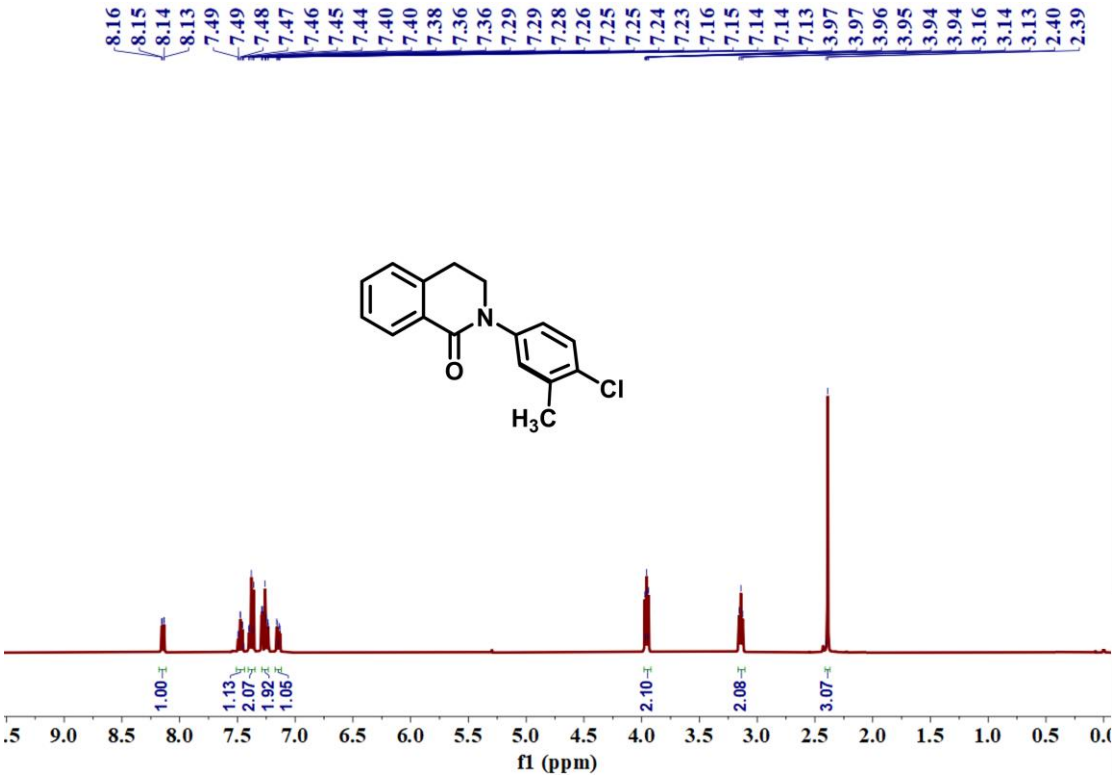

Fig. S25 ^{1}H NMR spectra of **2h** in $CDCl_3$.

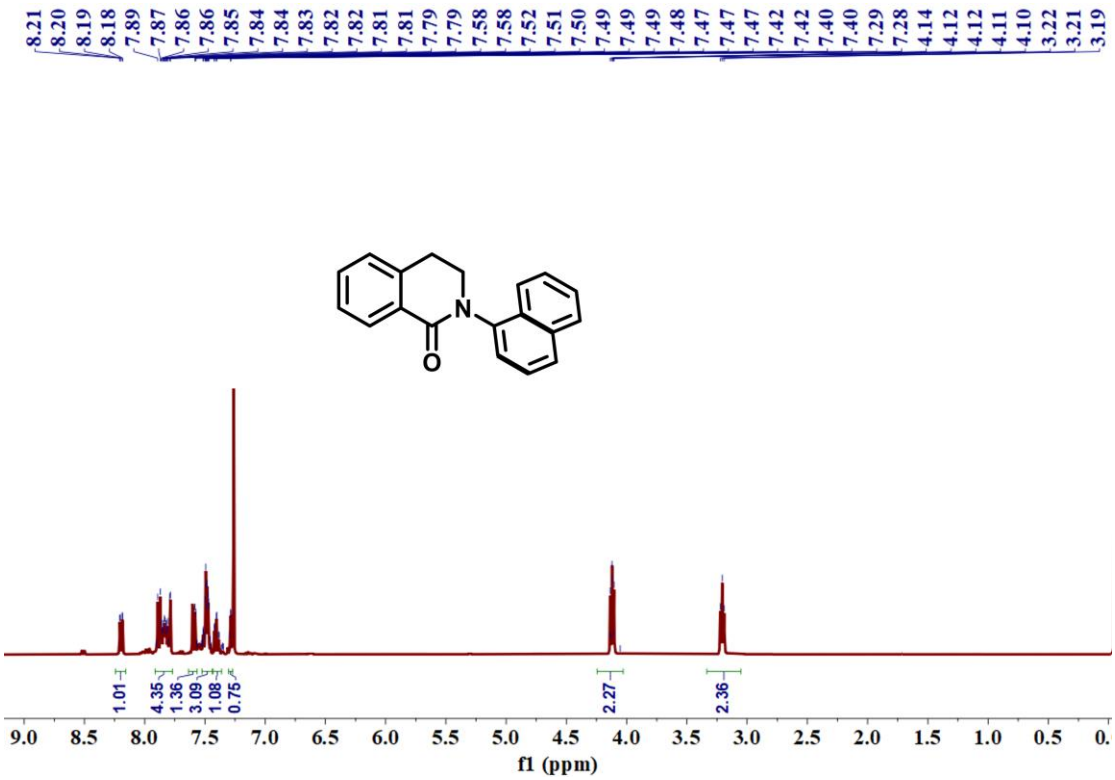

Fig. S26 ^{1}H NMR spectra of **2i** in $CDCl_3$.

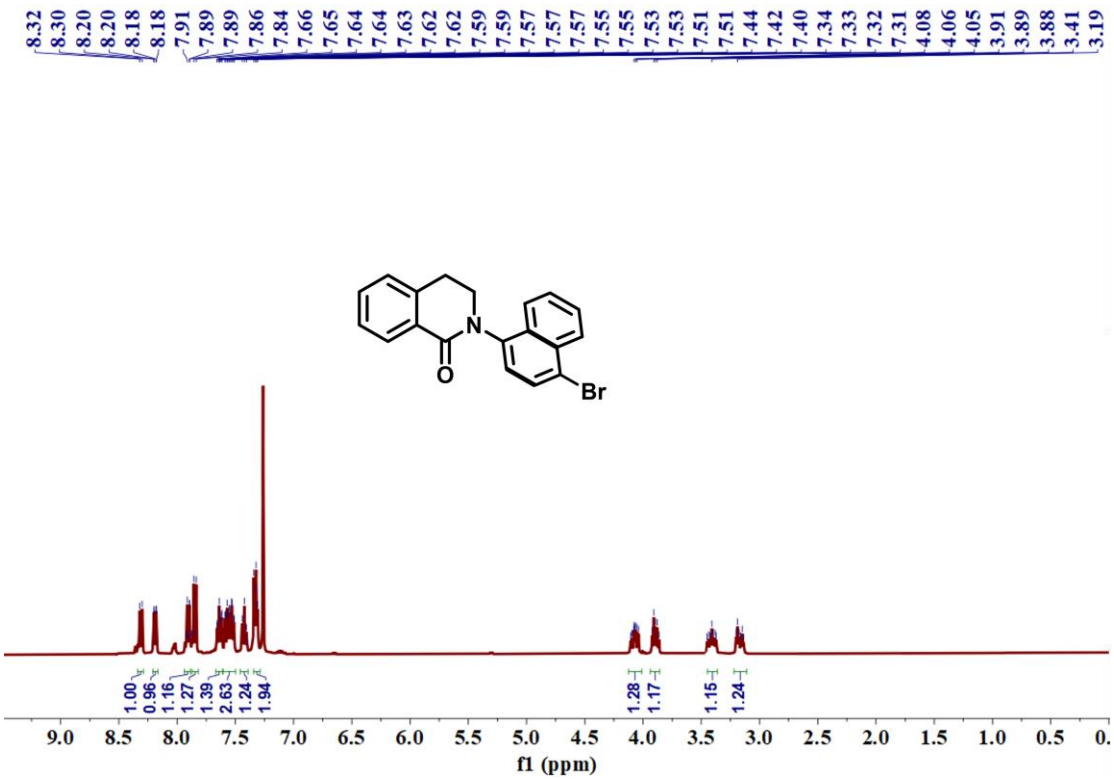

Fig. S27 ^{1}H NMR spectra of **2j** in $CDCl_3$.

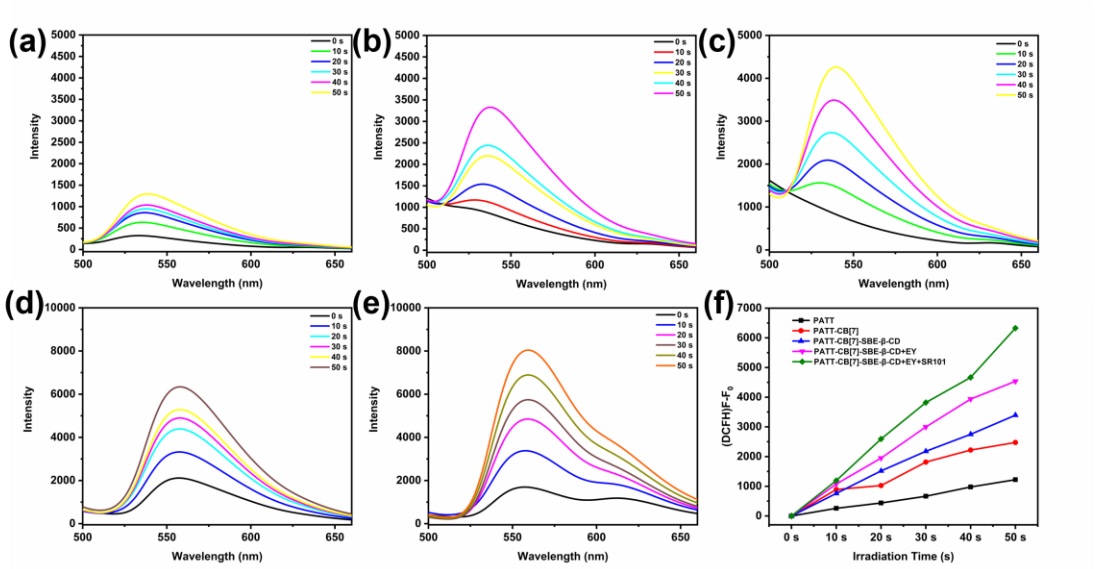

Fig. S28 The fluorescence spectra of DCFH (20 μM) after irradiation (360-365 nm) for different time in the presence of (a) PATT, (b) PATT-CB[7], (c) PATT-CB[7]-SBE-β-CD, (d) PATT-CB[7]-SBE-β-CD+EY, (e) PATT-CB[7]-SBE-β-CD+EY+SR101; (f) Plots of $\Delta F(F\text{-}F_0)$ of DCFH at fluorescence emission maxima upon light irradiation (365 nm) for different time intervals in the presence of PATT, PATT-CB[7], PATT-CB[7]-SBE-β-CD, PATT-CB[7]-SBE-β-CD+EY, PATT-CB[7]-SBE-β-CD+EY+SR101.

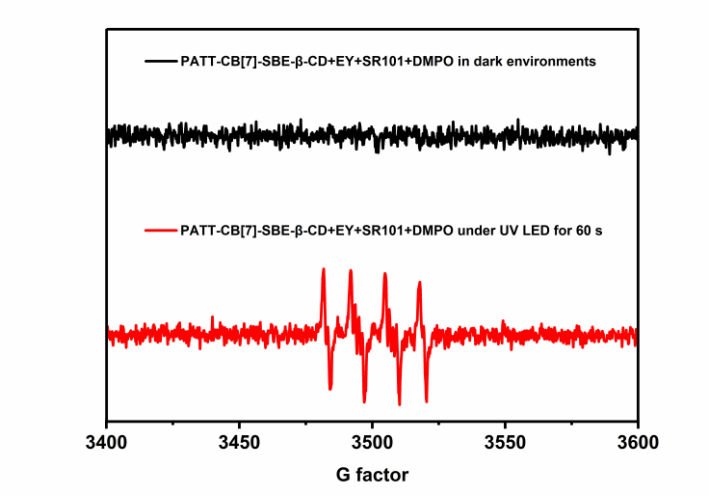

Fig. S29 EPR spectra of $O_2^{\bullet-}$ captured with DMPO as the trapping agent.

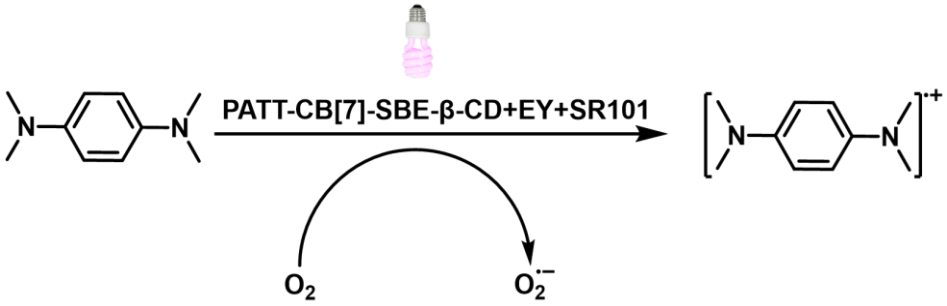

Fig. S30 The mechanism of TMPD as the $O_2^{\bullet-}$ indicator.

Table S1 photooxidative coupling reaction of benzylamine.[a,b]

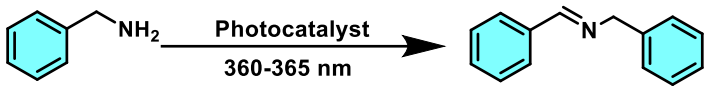

Entry	Variation from standard conditions [a]	Yield [b][%]
1	Standard condition	87
2	PATT-CB[7]	38
3	PATT-CB[7]-SBE-β-CD	46
4	PATT-CB[7]-SBE-β-CD+EY	63

[a]Standard conditions: benzylamine (0.2 mmol), PATT-CB[7]-SBE-β-CD+EY+SR101 (1 mol%), H_2O (2.0 mL), DIPEA (0.5 mmol), 360-365 nm LED, room temperature, 24 h; [b]Isolated yield.

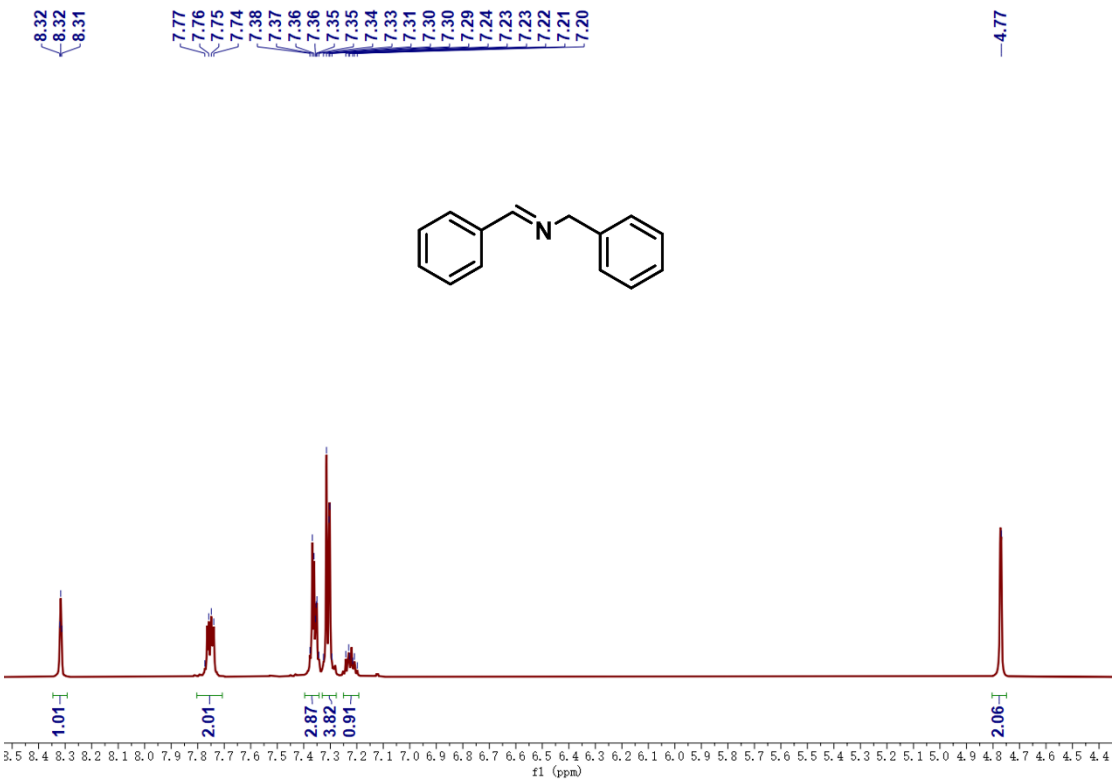

Fig. S31 ^{1}H NMR spectra of ***N*-benzyl-1-phenylmethanimine** in $CDCl_3$.

^{1}H NMR data of 2a-2j

2a. 2-Phenyl-3,4-dihydroisoquinolin-1(2H)-one

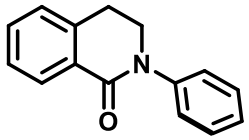

^{1}H NMR (400 MHz, $CDCl_3$) δ 8.15 (d, *J* = 7.7 Hz, 1H), 7.48-7.44 (t, *J* = 7.5 Hz, 1H), 7.37-7.33 (t, *J* = 7.6 Hz, 1H), 7.28-7.23 (q, *J* = 8.3 Hz, 6H), 3.97 (t, *J* = 6.4 Hz, 2H), 3.14 (t, *J* = 6.5 Hz, 2H).

2b. 2-(p-tolyl)-1,2,3,4-tetrahydroisoquinoline

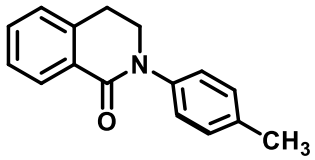

^{1}H NMR (400 MHz, $CDCl_3$) δ 8.16 (dd, *J* = 7.8, 1.4 Hz, 1H), 7.44 (m, *J* = 7.5, 1.5 Hz, 1H), 7.39 (m, *J* = 7.6, 1.3 Hz, 1H), 7.30-7.20 (m, 6H), 3.98-3.95 (m, 2H), 3.12 (t, *J* = 6.4 Hz, 2H), 2.42 (s, 3H).

2c. 2-(4-methoxyphenyl)-3,4-dihydroisoquinolin-1(2H)-one

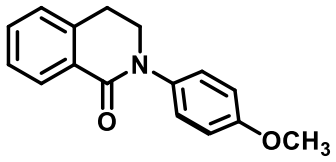

^{1}H NMR (400 MHz, $CDCl_3$) δ 8.16 (dd, *J* = 7.7, 1.4 Hz, 1H), 7.46 (d, *J* = 1.5 Hz, 1H), 7.37 (d, *J* = 1.2 Hz, 1H), 7.31-7.29 (m, 2H), 7.26-7.23 (m, 1H), 6.95-6.93 (m, 2H), 3.95-3.93 (dd, *J* = 7.0, 6.1 Hz, 2H), 3.86-3.83 (s, 3H), 3.15 (t, *J* = 6.5 Hz, 2H).

2d. 2-(4-fluorophenyl)-3,4-dihydroisoquinolin-1(2H)-one

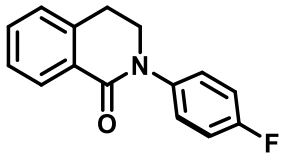

^{1}H NMR (400 MHz, $CDCl_3$) δ 8.16 (d, J = 1.6 Hz, 1H), 7.47 (d, J = 7.5 Hz, 1H), 7.41-7.33 (m, 3H), 7.24 (s, 1H), 7.15-7.07 (m, 2H), 3.98 (d, J = 6.2 Hz, 2H), 3.16 (d, J = 6.4 Hz, 2H).

2e. 2-(4-chlorophenyl)-3,4-dihydroisoquinolin-1(2H)-one

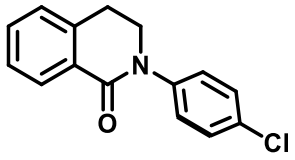

^{1}H NMR (400 MHz, $CDCl_3$) δ 8.08 (d, J = 1.6 Hz, 1H), 7.41 (d, J = 7.5 Hz, 1H), 7.33-7.28 (m, 5H), 7.27-7.19 (m, 1H), 3.92 (d, J = 6.2 Hz, 2H), 3.08 (d, J = 6.4 Hz, 2H).

2f. 2-(4-bromonaphthalen)-3,4-dihydroisoquinolin-1(2H)-one

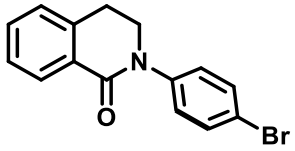

1H NMR (400 MHz, $CDCl_3$) δ 8.15 (dd, J = 7.8, 1.5 Hz, 1H), 7.60-7.24 (m, 9H), 4.02-3.93 (m, 2H), 3.15 (t, J = 6.4 Hz, 2H).

2g. 2-(p-nitrobenzene)-1,2,3,4-tetrahydroisoquinoline

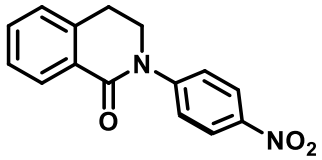

^{1}H NMR (400 MHz, $CDCl_3$) δ 8.30 (d, *J* = 8.6 Hz, 2H), 8.18 (d, *J* = 7.8 Hz, 1H), 7.63 (d, *J* = 8.7 Hz, 2H), 7.51 (t, *J* = 7.5 Hz, 1H), 7.44 (t, *J* = 7.8 Hz, 1H), 7.29 (d, *J* = 7.2 Hz, 1H), 4.09 (t, *J* = 6.4 Hz, 2H), 3.20 (t, *J* = 6.4 Hz, 2H).

2h. 2-(4-chloro-3-methylphenyl)-3,4-dihydroisoquinolin-1(2H)-one

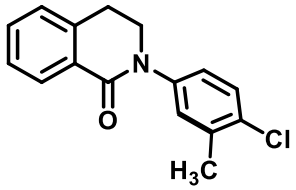

^{1}H NMR (400 MHz, $CDCl_3$) δ 8.14 (dd, *J* = 7.7, 1.4 Hz, 1H), 7.47 (td, *J* = 7.5, 1.5 Hz, 1H), 7.43-7.17 (m, 5H), 7.15 (dd, *J* = 8.5, 2.6 Hz, 1H), 3.96 (dd, *J* = 7.0, 6.0 Hz, 2H), 3.14 (t, *J* = 6.4 Hz, 2H), 2.39 (s, 3H).

2i. 2-(naphthalen-1-yl)-3,4-dihydroisoquinolin-1(2H)-one

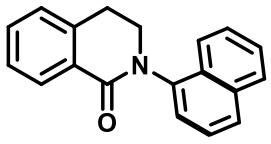

^{1}H NMR (400 MHz, $CDCl_3$) δ 8.19 (dd, *J* = 7.7, 1.5 Hz, 1H), 7.91-7.77 (m, 4H), 7.58 (d, *J* = 2.2 Hz, 1H), 7.52-7.44 (m, 3H), 7.40 (td, *J* = 7.6, 1.3 Hz, 1H), 7.29 (t, *J* = 1.6 Hz, 1H), 4.12 (dd, *J* = 7.0, 6.0 Hz, 2H), 3.21 (t, *J* = 6.4 Hz, 2H).

2j. 2-(4-bromonaphthalen-1-yl)-3,4-dihydroisoquinolin-1(2H)-one

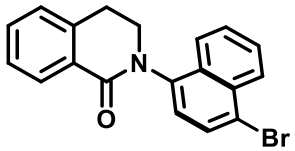

^{1}H NMR (400 MHz, $CDCl_3$) δ 8.31 (d, *J* = 8.4 Hz, 1H), 8.19 (dd, *J* = 7.7, 1.5 Hz, 1H), 7.95-7.81 (m, 2H), 7.75-7.49 (m, 3H), 7.47-7.28 (m, 3H), 4.07 (ddd, *J* = 12.3, 10.4, 4.6 Hz, 1H), 3.89 (dt, *J* = 11.9, 5.5 Hz, 1H), 3.41 (ddd, *J* = 15.8, 10.4, 5.2 Hz, 1H), 3.17 (dt, *J* = 15.9, 5.2 Hz, 1H).

***N*-benzyl-1-phenylmethanimine**

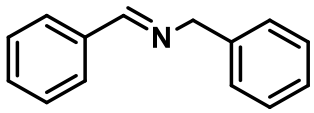

^{1}H NMR (400 MHz, $CDCl_3$) δ 8.32-8.31 (t, *J* = 1.5 Hz, 1H), 7.77-7.74 (m, 2H), 7.38-7.34 (m, 3H), 7.33-7.29 (m, 4H), 7.24-7.20 (m, 1H), 4.77 (s, 2H).